INSTITUTE OF PHYSICS PUBLISHING and INTERNATIONAL ATOMIC ENERGY AGENCY NUCLEAR FUSION

Nucl. Fusion **46** (2006) S416–S424 doi:10.1088/0029-5515/46/7/S04

Absorption of fast waves at moderate to high ion cyclotron harmonics on DIII-D

R.I. Pinsker, M. Porkolab[1], W.W. Heidbrink[2], Y. Luo[2], C.C. Petty, R. Prater, M. Choi, D.A. Schaffner[3], F.W. Baity[4], E. Fredd[5], J.C. Hosea[5], R.W. Harvey[6], A.P. Smirnov[6], M. Murakami[4] and M.A. Van Zeeland[7]

General Atomics, PO Box 85608, San Diego, California, 92186-5608, USA
[1] Massachusetts Institute of Technology, Cambridge, Massachusetts, USA
[2] University of California, Irvine, California, USA
[3] University of California, Los Angeles, California, USA
[4] Oak Ridge National Laboratory, Oak Ridge, Tennessee, USA
[5] Princeton Plasma Physics Laboratory, Princeton, New Jersey, USA
[6] CompX, Del Mar, California, USA
[7] Oak Ridge Institute for Science Education, Oak Ridge, Tennessee, USA

Received 7 November 2005, accepted for publication 9 March 2006
Published 14 June 2006
Online at stacks.iop.org/NF/46/S416

Abstract
The absorption of fast Alfvén waves (FW) by ion cyclotron harmonic damping in the range of harmonics from 4th to 8th is studied theoretically and with experiments in the DIII-D tokamak. A formula for linear ion cyclotron absorption on ions with an arbitrary distribution function which is symmetric about the magnetic field is used to estimate the single-pass damping for various cases of experimental interest. It is found that damping on fast ions from neutral beam injection can be significant even at the 8th harmonic if the fast ion beta, the beam injection energy and the background plasma density are high enough and the beam injection geometry is appropriate. The predictions are tested in several L-mode experiments in DIII-D with FW power at 60 MHz and at 116 MHz. It is found that 4th and 5th harmonic absorption of the 60 MHz power on the beam ions can be quite strong, but 8th harmonic absorption of the 116 MHz power appears to be weaker than expected. The linear modelling predicts a strong dependence of the 8th harmonic absorption on the initial pitch-angle of the injected beam, which is not observed in the experiment. Possible explanations of the discrepancy are discussed.

PACS numbers: 52.50.Qt, 52.40.Db, 52.50.Gj, 52.35.Bj, 52.55.Pi

(Some figures in this article are in colour only in the electronic version)

1. Introduction

A prerequisite for efficient fast wave current drive (FWCD) is that direct electron damping of the fast wave in the core of the plasma must dominate all other absorption mechanisms. Other damping mechanisms that may be important include ion cyclotron damping on either thermal or non-thermal populations resulting from neutral beam (NB) injection or alpha particles in a burning plasma, edge losses from far-field sheaths (reviewed by Myra [1]) or parametric decay instabilities (PDI) in the outer part of the plasma (discussed in this context by Wilson *et al* [2]). In the present work, we consider ion cyclotron harmonic damping on a fast ion population from NB injection, which has been shown to constitute an important power absorption mechanism in FWCD experiments on DIII-D [3]. The aim of this investigation is to compare observed ion cyclotron harmonic damping in DIII-D with theoretical predictions, in order to be able to quantitatively predict the power partition between direct electron damping and ion cyclotron damping for future applications of FWCD.

For the frequencies used for FWCD experiments in DIII-D (f = 60–120 MHz) and the range of toroidal fields used (B_T = 1.3–2.1 T), the cyclotron harmonic number is in the range f/f_{ci} = 4–12 for deuterium (half this for hydrogen). As is well known [4, 5], the fraction of the wave power absorbed by ion cyclotron damping as the fast wave propagates through a particular cyclotron harmonic layer in a slightly inhomogeneous magnetic field depends on the density of the absorbing ion species and the ratio of the wavelength of the fast wave $2\pi/k_\perp$ to the gyroradius $\rho_s = \sqrt{(\kappa T_s/m_s)}/(2\pi f_{cs})$ of the absorbing ion species s. This ratio may be expressed

as $k_\perp \rho_s$, and typical numerical values range from $k_\perp \rho_s \sim 0.1$ for thermal hydrogen at the 2nd harmonic at $B_T = 2\,T$ to $k_\perp \rho_s \sim 4$ for absorption on an injected deuterium beam at the 8th harmonic at $B_T = 1\,T$.

The outline of the paper is as follows. The first part addresses the linear theory of ion cyclotron absorption in a uniform magnetized plasma, with either isotropic Maxwellian velocity distributions or with an anisotropic slowing-down distribution. While ignoring the self-consistent effect of the fast Alfvén waves (FW) power on the ion distribution, such a linear estimate of the damping strength may be appropriate for situations where the effect of the NB power on the ion distribution function is much larger than that of the FW power. The most important effect of relaxing the uniform plasma assumption can be addressed with ray tracing, so a brief discussion of the characteristics of fast wave ray trajectories follows. The latter part of the paper constitutes a short survey of recent experiments in DIII-D in which ion cyclotron harmonic absorption on injected beams was studied at two FW frequencies and at various harmonic numbers.

2. Theory

2.1. Formulae for linear ion cyclotron absorption

Porkolab has given a formula for the optical depth due to ion cyclotron absorption of the fast wave on a hot ion species (designated with the subscript s) [5]:

$$2\eta = \frac{\pi}{2}\left(\frac{n_{hot}}{n_i}\right)\left(\frac{\omega_{pi} R_M}{c}\right)(\ell-1)^2 e^{-\lambda_s} \times \left\{ I_{\ell-1}(\lambda_s) + \frac{\lambda_s}{\ell}[I_\ell(\lambda_s) - I_{\ell-1}(\lambda_s)] \right\}, \quad (1)$$

in which the argument of the modified Bessel functions is $\lambda_s \equiv (1/2)(k_\perp \rho_s)^2$, the ion cyclotron harmonic is $\ell = f/f_{cs} = \omega/\Omega_s$, ω_{pi} is the ion plasma frequency for the bulk ions, n_{hot} and n_i are the densities of the hot and bulk (thermal plus hot) ion species and R_M is the major radius of the ion cyclotron resonance layer (assuming the magnetic field strength satisfies $R_M B_0 =$ constant). The optical depth is defined by the power transmission coefficient for one traversal of the cyclotron resonance layer of $T = \exp(-2\eta)$ and hence a fraction $A = 1 - T$ of the incident power absorbed there. (Note that for $2\eta \ll 1$, $A \approx 2\eta$.) The following assumptions were used in the derivation of equation (1)

1. The hot species is taken to have an isotropic Maxwellian distribution; several authors have examined the effect of relaxing this assumption, as in [6], and we will also do this in the following.
2. Only the left-circularly polarized component of the wave electric field is retained, which is a good approximation for absorption at the fundamental ion cyclotron resonance.
3. The simplest cold-plasma forms of the fast wave dispersion ($\omega^2 = k_\perp^2 V_A^2$, where V_A is the Alfvén velocity) and polarization [$|E_+|^2/|E_y|^2 = (\ell-1)^2$] have been used, and the effect of non-zero $k_\parallel$ has been neglected.

Arbitrarily large values of $k_\perp \rho_s$ are correctly treated in equation (1).

While continuing to treat the absorbing ion species as having an isotropic Maxwellian distribution for the moment (assumption #1), we have relaxed simplifying assumptions #2 and #3 to obtain the following more complete form for this optical depth. The resulting expression is

$$2\eta = R_M \frac{\ell \omega_{ps}^2}{4 n_\perp f c} e^{-\lambda_s}\left[\left(\frac{R - n_\parallel^2}{S - n_\parallel^2}\right)^2 \Delta_-^\ell(\lambda_s) + \left(\frac{L - n_\parallel^2}{S - n_\parallel^2}\right)^2 \times \Delta_+^\ell(\lambda_s) + \frac{2\lambda_s}{\ell}\{\Delta_+^\ell(\lambda_s) - \Delta_-^\ell(\lambda_s)\}\right], \quad (2)$$

in which the cold plasma Stix symbols for a multi-ion species plasma R, L and S have their usual definitions [4], the frequency $f = \omega/(2\pi)$ and the combinations of modified Bessel functions have the definitions $\Delta_+^\ell(x) \equiv I_\ell(x) - I_{\ell+1}(x)$ and $\Delta_-^\ell(x) \equiv I_{\ell-1}(x) - I_\ell(x)$. The perpendicular index of refraction for the FW, $n_\perp = k_\perp c/\omega$, can either be taken from a solution of the full local dispersion relation or the cold plasma approximation in which the slow and FWs have been decoupled can be used, which (introducing the Stix symbol D) yields $n_\perp^2 \approx \lfloor D^2 - (n_\parallel^2 - S)^2 \rfloor/(n_\parallel^2 - S)$.

In the derivation of equation (2), the assumption of isotropic Maxwellian ion distribution functions was retained. Non-zero parallel wavenumber is accounted for, and the contributions to the damping from the left-hand circularly polarized (the first term in the square bracket), right-hand circularly polarized (the second term in the bracket) and the cross-terms are all included. Although in the limit of small $\lambda_s \ll 1$ the E_+ (left-hand circularly polarized) term is dominant in the square bracket, the E_- (right-hand circularly polarized) term increases more quickly with λ_s so that at some value of λ_s it becomes larger in magnitude than the E_+ term. This is illustrated in figure 1, in which the three terms in the square bracket are compared as a function of λ_s for 2nd and 6th harmonics. It is evident that treating only the E_+ contribution (as in equation (1)) considerably underestimates the ion cyclotron damping for large values of λ_s. The contribution due to the third term in the square bracket, which results from the residual linear polarization, is small for moderate to high harmonic numbers.

Using an isotropic Maxwellian to model the fast ion distribution function resulting from NB injection (simplifying assumption #1) neglects two critical aspects of a realistic slowing-down distribution function (SDDF). Most importantly, while the SDDF has almost no particles at energies higher than the sum of the injection energy and the electron temperature, the Maxwellian is non-zero for arbitrarily high energies. The strength of the wave/particle interaction as a function of perpendicular energy is peaked at an energy which increases rapidly with harmonic number, so that at high harmonics practically all of the damping occurs on the most energetic particles present in the distribution. Hence, using a Maxwellian (that lacks the high-energy cutoff near the injection energy) leads to a significant overestimate of the damping and that overestimate grows with the harmonic number. Secondly, for injection energies higher than the critical energy at which the slowing-down occurs equally on electrons and ions, the initial slowing down is not accompanied by appreciable pitch-angle scattering. The damping at high

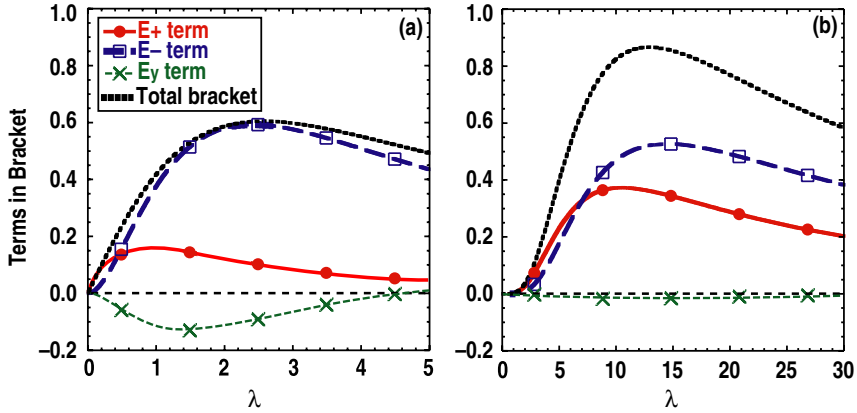

Figure 1. Comparison of terms in the square bracket of equation (2) for the (*a*) 2nd harmonic and (*b*) 6th harmonic. Note that the E_+ term dominates only at small values of λ.

harmonics occurs primarily on ions that retain their birth pitch-angle, so that the important part of the distribution function is highly anisotropic.

In order to evaluate the optical depth for a single ion cyclotron harmonic layer with an arbitrary zero-order ion distribution function which is symmetric about the magnetic field, we further generalize equation (2). This is done by evaluating Stix's expression [4] for the absorbed power, Stix's equation (11–69), for a general distribution function in a uniform non-relativistic magnetized plasma assuming $E_\parallel = 0$, using the imaginary parts of the susceptibility tensor in Stix's equation (10–45) and equation (10–56), then dividing by the Poynting flux as described by Porkolab [5], in which nearly radial propagation near the cyclotron resonance layer is assumed and the wave polarization is being determined by the local values of the cold plasma dielectric tensor elements (thereby neglecting mode conversion), and finally obtaining

$$2\eta = R_{\rm M}\frac{\pi\omega_{\rm ps}^2}{f c n_\perp}\int_{-\infty}^{+\infty} {\rm d}u_\parallel \int_0^\infty {\rm d}u_\perp u_\perp^2 \times \left(\left[\frac{D}{S-n_\parallel^2}\right]\frac{\ell J_\ell(\alpha u_\perp)}{\alpha u_\perp} + J_\ell'(\alpha u_\perp)\right)^2 (-\mathscr{D}_u f_0)\,. \qquad (3)$$

The velocity distribution has been normalized so that $\iiint {\rm d}^3\boldsymbol{u}\, f_0(\boldsymbol{u}) = 1$ and the differential operator $\mathscr{D}_u$ is defined as

$$\mathscr{D}_u \equiv \left(\frac{\ell\Omega_s}{\omega}\right)\frac{\partial}{\partial u_\perp} + \frac{u_\perp}{\xi}\frac{\partial}{\partial u_\parallel}.$$

In these equations, velocities have been normalized to a convenient speed $V_{\rm norm}$, such as the thermal velocity for a Maxwellian or the beam injection speed $V_{\rm b}$ for a slowing-down distribution, α is defined by $\alpha \equiv k_\perp V_{\rm norm}/\Omega_s$ and ξ is the normalized wave parallel phase velocity $(\omega/k_\parallel)/V_{\rm norm}$. For a non-relativistic beam ($V_{\rm b}/c \ll 1$) the parameter ξ is usually large compared with unity and the differential operator $\mathscr{D}_u$ near the resonance layer $\omega = \ell\Omega_s$ for $u_\perp$ less than or not much greater than $V_{\rm b}$ reduces to approximately the (normalized) perpendicular derivative (i.e. $\mathscr{D}_u \approx \partial/\partial u_\perp$).

For distributions written more naturally in spherical velocity space coordinates (u, θ), where $u^2 = u_\perp^2 + u_\parallel^2$ and $\theta = \tan^{-1}(u_\perp/u_\parallel)$, the double integral in velocity space that gives the optical depth can be rewritten as

$$2\eta = R_{\rm M}\frac{\pi\omega_{\rm ps}^2}{f c n_\perp}\int_0^\pi \sin^2\theta\,{\rm d}\theta \left\{\int_0^\infty u^3\,{\rm d}u \left(\left[\frac{D}{S-n_\parallel^2}\right] \times \frac{\ell J_\ell(\alpha u\sin\theta)}{\alpha u\sin\theta} + J_\ell'(\alpha u\sin\theta)\right)^2 (-\mathscr{D}_u f_0)\right\} \qquad (4)$$

and the differential operator $\mathscr{D}_u$ can be expressed in spherical coordinates using

$$\frac{\partial}{\partial u_\parallel} = \cos\theta\frac{\partial}{\partial u} - \frac{\sin\theta}{u}\frac{\partial}{\partial\theta}$$

and

$$\frac{\partial}{\partial u_\perp} = \sin\theta\frac{\partial}{\partial u} + \frac{\cos\theta}{u}\frac{\partial}{\partial\theta}.$$

Comparing equations (2) (valid only for a Maxwellian f_0) and (4), it can be seen that the term in the square that does not have a factor involving the Stix symbols D and S is the one related to the linear polarization $|E_y|^2$ and that the two circular polarization terms in equation (2) are mixed together in the other term in the square in equation (4). In the case where f_0 is an isotropic Maxwellian one can explicitly perform the integration in equation (3) and obtain equation (2).

To model the SDDF resulting from NB injection, the standard asymptotic solution of the Fokker–Planck equation given by Cordey and Core [7] is used, in which the pitch-angle dependence of f_0 is expanded in Legendre polynomials. Only the full energy component of the beam is considered, and the distribution of initial pitch-angles is taken to be Gaussian, as in [6], assuming the mean initial pitch-angle is determined by the injection geometry, and the volume of interest is near the magnetic axis in the tokamak midplane. For energies above the injection energy, the distribution function decays exponentially with a tail width proportional to the electron temperature [6, 7]. However, the width of this tail can be significantly larger than the electron temperature due to the effects of the dc toroidal electric field and ion–ion collisions among the beam particles [7]. Also the effect of rf absorption is to increase the width of this tail [8]. The absorption at moderate to high harmonics is strongly peaked in just this part of the distribution function. We can get a qualitative idea of the effect on the optical depth of all these tail-widening effects

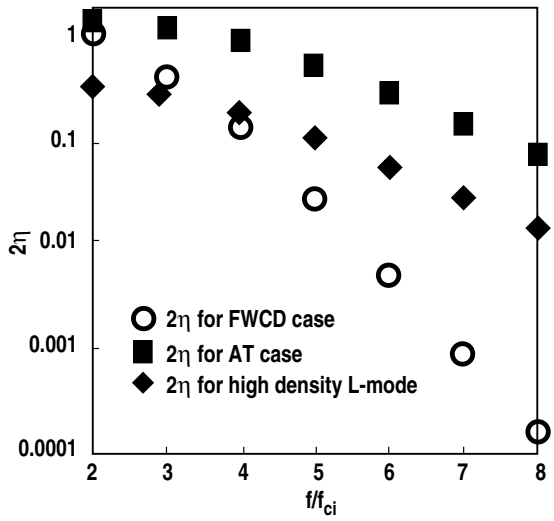

Figure 2. Predicted optical depth for absorption on fast ions from 2nd to 8th harmonic for three different sets of plasma parameters given in the text. In all three cases, the initial pitch-angle of the fast ions is taken to be a Gaussian distribution with mean of 50° (to model 'left' source injection on DIII-D) and a width of about 7° (0.12 rad).

by artificially increasing the width of the tail above the value given by the electron temperature.

This locally uniform plasma model neglects trapped particles, orbit effects and other manifestations of the inhomogeneous magnetic field. It is assumed that the cyclotron harmonic resonance layer is positioned so that the magnetic axis lies in that resonance layer, and all quantities are evaluated at the magnetic axis. The distribution of birth pitch-angles is modelled with a Gaussian, as in [6]. The mean of the birth distribution of pitch-angles is 50° for the DIII-D 'left' sources (the more tangential of the two injection angles) and 65° for DIII-D 'right' sources. The width of the initial pitch-angle distribution is taken to be 7°; the results are not sensitive to the exact value taken. Values of $\mathscr{D}_u f_0$ in the (u, θ) plane are evaluated numerically, as is the double integral in equation (4).

2.2. Evaluation of linear cyclotron damping for DIII-D experimental conditions

This numerical evaluation of equations (2) and (4) has been used to estimate the single pass damping for three different conditions used in DIII-D FW experiments. In figure 2, a comparison is presented of the optical depth 2η for three different cases at a fixed magnetic field of 1.97 T. The first condition, from the FWCD study reported in [9], is a 1.1 MA low density [$n_e(0) = 2.6 \times 10^{13}\,\mathrm{cm}^{-3}$] L-mode discharge with 2.7 MW of 80 keV deuterium NB injection from a 'left' source (initial pitch-angle of 50°). The central fast ion density was $n_f = 1.5 \times 10^{13}\,\mathrm{cm}^{-3}$, as derived from modelling with the ONETWO transport code [10]. We consider the harmonic number range $\ell = 2, 3, \ldots, 7, 8$. In agreement with the conclusions of [9], the predicted 8th harmonic absorption is negligible, while the ~13% single pass damping ($2\eta = 0.14$) predicted at 4th harmonic is comparable to the expected direct electron absorption. Using the simpler 'effective Maxwellian' model embodied in equation (2), in which we use the effective temperature for the beam derived from ONETWO, $T_{\mathrm{eff}} \equiv (2/3)W_f/n_f$ in which W_f is the stored energy density in the fast ions, we find similar results: ~18% single pass absorption at 4th harmonic and negligible 8th harmonic absorption. The simplest approximation (equation (1)) yields ~20% single pass damping ($2\eta = 0.22$) at 4th harmonic and about 1% single pass damping at 8th harmonic.

The second case is representative of H-mode advanced tokamak (AT) discharges with 9.8 MW of NB power in which central FWCD is desired for control of the central safety factor, q_0. The parameters are taken from an experimental case that was run without FW power; the central density in this discharge was $n_e(0) = 6.3 \times 10^{13}\,\mathrm{cm}^{-3}$ and the central fast ion density was $n_f = 0.95 \times 10^{13}\,\mathrm{cm}^{-3}$. The higher central density yields values of the argument of the Bessel functions for the fast particles λ_f that are about 2.5 times higher than in the low-density case for a given harmonic, and this results in substantially higher absorption for $\ell \geqslant 3$ despite the lower fast ion density. Furthermore, the decrease in absorption with increasing harmonic number is slower, so that the model predicts ~7.5% single-pass absorption ($2\eta = 0.078$) at the 8th harmonic. In this case the 'effective Maxwellian' model (equation (2)) substantially overestimates the 8th harmonic damping, with ~30% single-pass absorption predicted. Degradation in the FWCD efficiency due to cyclotron absorption on the beam is possible if the direct electron absorption is weak compared with the absorption on the fast ions, which would certainly be expected for the 4th harmonic case.

The third case is from a recent experiment, discussed in more detail below, in which FW absorption at 4th and 8th harmonics was studied in a high density L-mode with 5.0 MW of NB heating. The central electron and fast ion densities were $n_e(0) = 6.8 \times 10^{13}\,\mathrm{cm}^{-3}$ and $n_f = 0.26 \times 10^{13}\,\mathrm{cm}^{-3}$. Since the central density and beam energy were about the same as in the high density H-mode case, the values of λ_f and the dependence of the absorption on ℓ were similar in the two cases. The single-pass absorption is lower owing to the lower fast ion density in the L-mode case, which in turn stems from the lower electron temperature and lower beam power in the L-mode case. While the predicted single-pass absorption at 4th harmonic, 28% ($2\eta = 0.33$), is still very substantial, the 8th harmonic single-pass absorption is reduced to 4% ($2\eta = 0.041$), which is similar in magnitude to the edge losses that have been inferred in low current L-mode plasmas in previous studies [11]. Hence, in this experimental condition 8th harmonic cyclotron absorption might be only marginally observable in the face of comparable edge losses and comparable central direct electron absorption.

One aspect of damping on the SDDF that cannot be addressed with the isotropic Maxwellian model is the dependence of the damping strength on the initial pitch-angle, which is determined by the beam injection geometry. From inspection of equation (3) or (4), one expects that for a given injection energy the strongest high harmonic damping will occur for perpendicular injection. This is illustrated in figure 3, where the expected optical depth for the 4th and 8th harmonics has been calculated for the plasma parameters of the third (high-density L-mode) case. For both harmonics, the optical depth increases rapidly with birth pitch-angle in the ~45°

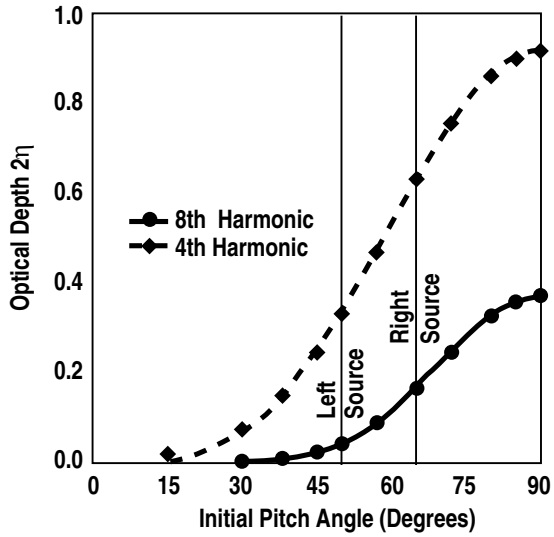

Figure 3. Predicted optical depth for absorption on fast ions for 4th and 8th harmonic as a function of the initial pitch-angle. The plasma parameters are the same as in the high-density L-mode case in figure 2, and the assumed width of the distribution of birth pitch-angles is again 0.12 rad. The vertical lines show the initial pitch-angle associated with the DIII-D 'left' and 'right' sources.

to 75° region, so that one expects an observable increase in absorption in changing from 'left' to 'right' sources.

2.3. Ray propagation effects on cyclotron damping

These estimates have been made with a zero-dimensional model for wave propagation. To determine the corrections due to the effects of propagation in an inhomogeneous toroidal equilibrium, the GENRAY ray-tracing code has been used [12]. One very important correction results from the evolution of $n_\parallel$ along the ray trajectory (beyond the $1/R$ dependence due to the conservation of toroidal mode number), which in turn stems from the non-constancy of the wave's poloidal mode number along the ray trajectory and the magnetic shear. As the ray propagates, the polarization factors in equation (2) or the $D/(S - n_\parallel^2)$ factor in equations (3) and (4) and hence the strength of the damping upon traversing a resonance layer are strongly affected by the local $n_\parallel$. Also the value of the perpendicular wavenumber, and hence the argument of the Bessel functions, increases with decreasing $n_\parallel$. Since the Stix parameter S is negative within the bulk of the plasma, both these effects are in the same direction: increased cyclotron damping as the magnitude of $n_\parallel$ decreases. This phenomenon largely explains the differences in damping seen in the ray-tracing results from different crossings of a given resonance, even at comparable normalized radii. A number of such resonance traversals have been examined in detail [12], and the linear ion cyclotron resonance damping from GENRAY (which should be equivalent to equation (2)) is indeed found to be in good agreement with the results of equation (2) in which the local values of $n_\parallel$ and $n_\perp$ are used.

Another aspect of fast wave ray propagation that has been studied with the GENRAY code is the tendency of the fast wave to evolve from a compressional Alfvén wave dispersion $\omega^2 \approx (k_\perp^2 + k_\parallel^2)V_A^2$ (where V_A is the Alfvén speed) at low harmonics to a whistler-like dispersion at high harmonic. As discussed by Ikezi *et al* [13], as the harmonic number increases above three or four, the range of $n_\parallel$ for which the angle between the group velocity vector and the static magnetic field exceeds the well-known limit of 19.5° [4] for whistlers shrinks to only a small region around $n_\parallel = 0$. The resulting tendency of the fast wave rays at high harmonics to duct along the static magnetic field and radially penetrate only slowly is somewhat reminiscent of the familiar resonance-cone behaviour of lower-hybrid waves. We have computationally verified this property of the ray trajectories in the high harmonic regime. In some cases at high harmonics, the ray paths can curve so strongly in poloidal cross-section that the fast wave power does not reach the major radius of the cyclotron resonance layer or the $n_\parallel$ of the wave at the crossing of the resonance can be substantially different from the launched value which in turn strongly affects the polarization and absorption there.

3. Experiments

3.1. Results

DIII-D experiments performed in 1998–1999 demonstrated strong damping of 60 MHz FW power on beam ions at the 4th harmonic [14]. The acceleration of beam ions by the rf power was observed directly with active neutral particle charge exchange analyzers and indirectly from enhanced fusion neutron emission and from force balance calculated through equilibrium reconstruction. 5th harmonic absorption of FW power at 83 MHz was found to be relatively weak. In the 4th harmonic case, intentional introduction of a thermal hydrogen minority of more than about $n_H/(n_H + n_D) > 5\%$ decreased the power absorbed by the deuterium beam ions, as the strong 2nd harmonic absorption on the hydrogen reduces the power available to the deuterium.

Recent DIII-D experiments extended these results in several directions. In the same 60 MHz, $\ell = f/f_{cD} = 4$ regime of the earlier work, a new diagnostic technique was used to observe the rf-driven acceleration of the deuterium beam ions. The technique, described in [15], is based on observation of the Doppler-shifted D_α spectrum from the charge exchange between the fast ions and the injected NB. The spectra observed using this diagnostic indicate acceleration of the beam above the injection energy, and the fast ion tail correlates with enhanced neutron emission. Detailed observations with this diagnostic of the effect of the 4th harmonic acceleration on the beam will be presented in a forthcoming publication.

DIII-D deuterium discharges in general have a background hydrogen fraction of $H/D < 2\%$. To demonstrate that residual (thermal) hydrogen absorption at half the harmonic number does not play a dominant role in the 4th harmonic case at this low level of n_H/n_D, a condition was studied in which the $\ell = 5$ deuterium harmonic for $f = 60$ MHz passed through the magnetic axis and no hydrogen harmonic was present in the core of the discharge. This condition was otherwise similar to the 4th harmonic condition studied in [14], with the equivalent of 1.2 MW of 80 keV NBs and 0.8 MW of coupled 60 MHz FW power. Time histories from this discharge are shown in figure 4. The neutron emission rate is compared with the predicted rate based on a zero-dimensional

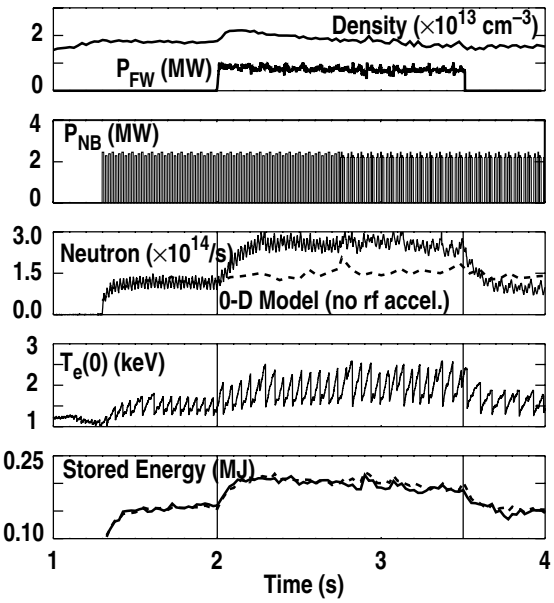

Figure 4. Time history of low-density L-mode discharge with 5th harmonic heating (60 MHz, $B_T = 1.55$ T). The two small disturbances in the stored energy, central electron temperature and density around 3 s are due to 'dithers' into H-mode.

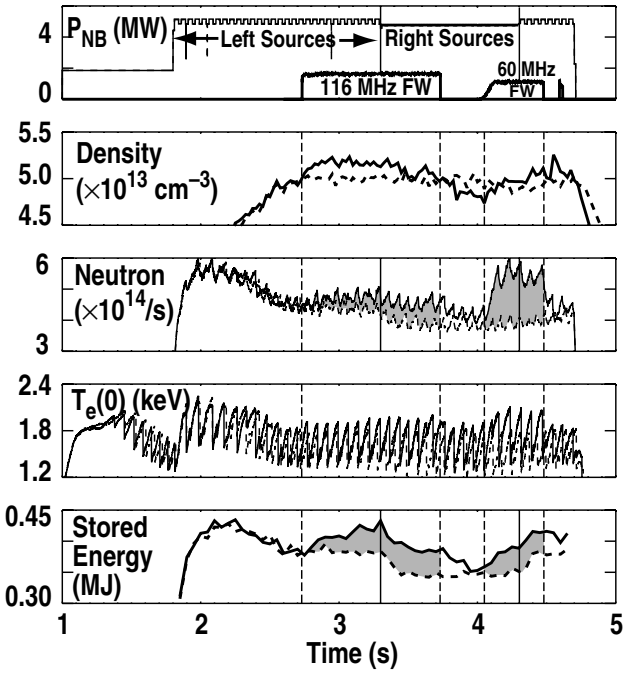

Figure 5. Time history of high density L-mode discharge comparing 4th (60 MHz) and 8th harmonic (116 MHz) FW heating at 1.85 T. Dotted vertical lines show rf on and off times; solid vertical lines demarcate the periods where 'left' ($R_{tan} = 115$ cm) and 'right' ($R_{tan} = 76$ cm) ion sources are used. Dashed traces are from comparison case with no FW.

model [14] that includes classical beam slowing-down physics and uses measured plasma parameters but does not include acceleration of the beam. The model successfully predicts the neutron rate before and after the FW power is injected, but the neutron emission rate is enhanced by a factor of 2.0 (as defined in [14]) during combined FW and NB injection. This result is confirmed by more sophisticated calculations using the measured profiles in the ONETWO and TRANSP [16] codes. The value of the neutron enhancement is comparable to that obtained in the best cases with 60 MHz at 4th harmonic (at 1.25 times higher magnetic field) in otherwise very similar plasma conditions. The single-pass absorption predicted by either equation (2) or equation (4) at 5th harmonic in this case is about double of what is predicted for 4th harmonic at the same FW frequency; the higher value of λ_s at the lower magnetic field more than compensates for the decrease in the Bessel functions with increasing order at fixed values of the argument. This is not inconsistent with [14], where it was concluded that 5th harmonic absorption was weak compared with 4th, because that conclusion referred to comparison at fixed magnetic field and with varying the frequency.

In contrast to a comparison of absorption at different harmonics at fixed FW frequency, it was shown in figure 2 that the single-pass absorption indeed decreases rapidly with increasing harmonic number when the magnetic field is fixed. While the low density L-mode FWCD studies reported in [9] showed experimentally that the 8th harmonic absorption was negligible compared with 4th harmonic at ∼2 T, one expects that the slower decline in absorption with harmonic number associated with higher values of λ_s, obtained at higher plasma densities, could lead to observable 8th harmonic absorption under both high density L-mode and H-mode conditions, as discussed in the previous section. An experiment was carried out to test this, in which a high density beam-heated L-mode was used as the target plasma and FW power was coupled both at 60 MHz and 116 MHz. L-mode was chosen in order to maximize the coupled FW power (higher antenna loading resistance and corresponding low antenna voltages.) The relatively low electron temperature (compared with H-mode) and the shorter slowing-down time led to a lower fast ion density in the high density L-mode case and hence the smaller single-pass absorption described above. The predicted single-pass absorption at 8th harmonic, 116 MHz is about 4% per pass for the beam injection geometry of a 'left' source, while the absorption is predicted to be about 15% per pass for a 'right' source. Again, the optical depth is sensitive to the value of $n_\parallel$ at the traversal of the resonance; a value of $n_\parallel = 4$ has been taken for this estimate. The predicted value of the optical depth for the 'right' source case is similar to that predicted for a 'left' source in the 5th harmonic, 60 MHz case discussed above. Hence, the fact that efficient absorption and accompanying neutron enhancements were seen in the 5th harmonic case with a 'left' source implies that signs of strong absorption could be expected for both the 4th and 8th harmonic absorption in the high density L-mode condition if a 'right' source is used. While absorption at the 4th harmonic should remain strong with a 'left' source (single-pass absorption of about 28%), absorption at the 8th harmonic might not be observable with a 'left' source, since the single-pass absorption due to direct electron damping and to edge losses might be comparable to or larger than the ion cyclotron harmonic absorption (4% per pass).

These expectations are only partially borne out in the experimental result, shown in figure 5, where the time history

of a discharge with coupled FW power levels of 1.6 MW at 116 MHz and 1.1 MW at 60 MHz is compared with a reference shot with no FW power. The NB injection angle is changed from 'left' to 'right' (i.e. from an initial pitch-angle of 50° near the magnetic axis to 65°) at 3.3 s, which is midway through the 116 MHz pulse, then switched back from 'right' to 'left' during the 60 MHz pulse. Although a substantial neutron enhancement (∼1.4 in comparison with the reference shot) is seen for the 60 MHz power for either beam injection angle, only a very small enhancement at either beam angle is seen for the 8th harmonic heating at 1.45 times higher FW power. The increment in stored energy is comparable for the two FW frequencies, despite the difference in power levels. The increase in stored energy due to the 116 MHz power appears across the electron and ion temperature profiles, while the deposition of the 60 MHz power is more centrally peaked. No evidence of a strong increase in the interaction of the 116 MHz power with the beam ions is seen at the switchover from 'left' to 'right' sources at 0.57 s into the 116 MHz pulse, although there appears to be a slightly larger difference between the neutron rate with and without 116 MHz power in the expected direction at that switchover.

3.2. Discussion

The principal difficulty in comparing the experimental results with theoretical expectations is that for rf pulses longer than the Alfvén transit time (a fraction of a microsecond for DIII-D parameters), only the global absorptivity of the plasma is observable, which is the net effect of multiple passes of the waves through the absorbing region. The fraction of the applied rf power that is absorbed in the core is determined by the balance between the single pass absorption in the core and the loss per bounce at the plasma edge. In general the edge losses are not well characterized, and the theory predicts only the core single pass absorption. For this reason, the emphasis in this experiment was to compare different harmonics and different beam injection geometries, under the assumption that the edge losses were essentially unchanged under these variations.

With these caveats, we proceed to discuss possible explanations for the apparent discrepancy between the linear theory, which predicts a jump in absorption from an only marginally observable level with a 'left' source to a fairly strong absorption for the 'right' source for the 8th harmonic in this case, and the experimental result, which gave little evidence for strong central absorption at either beam injection angle at the 8th harmonic. Although an anomalously high rate of pitch-angle scattering might account for the weak dependence of the 8th harmonic absorption on the injected pitch-angle, measurements of pitch-angle scattering of beam ions in DIII-D [17] were shown to be consistent with the classical theory (in a low density regime, however). Perhaps more significantly, the dependence of the high harmonic absorption on injected pitch-angle shown in figure 3 would suggest that if there were an anomalously high rate of pitch-angle scattering, the single pass absorption with left source injection would be increased to a significant level while the absorption with right source injection would be decreased somewhat, while remaining at a significant level. Instead, what the experiment suggests is an unexpectedly low level of absorption at both pitch-angles.

Possible rf-specific explanations for the discrepancy include the following.

(1) There could be strong edge losses for both frequencies in this high density L-mode condition, so that the edge losses dominate the weaker 8th harmonic absorption and only reduce the central 4th harmonic absorption.
(2) The 8th harmonic may suffer from losses that are stronger than those at the 4th harmonic, e.g. edge-localized parametric decay such as observed in a similar regime in NSTX ([2]).
(3) The linear theory with a uniform plasma model may be inadequate in this situation.

The argument for the first possibility would be that DIII-D FWCD experiments in ELMing H-modes [18] showed that when the edge plasma density is high enough due to high ELM frequency, high antenna loading is correlated with the loss of efficient multiple-pass absorption. Hence, the high antenna loading observed in the high density L-mode condition of the discharge shown in figure 5 might similarly correspond to a relatively high edge loss. It was possible to infer the edge loss that would be required to account for the FWCD results in [18] from measurements of the driven central current. The higher central density and lower central electron temperature in the present case mean that a similar measurement of FWCD would be very much more difficult because of the smaller driven current.

The second possibility (that edge losses might be greater for the higher frequency FWs) can be investigated by comparing PDI in both 4th and 8th harmonic cases. Strong PDI and evidence for significant power absorption with high harmonic fast wave launch has been recently reported from NSTX [2] at somewhat higher, but comparable, harmonic number. Although a detailed study of PDI in the DIII-D experiments has not yet been performed, PDI spectra have been observed in the 8th harmonic case with high frequency probes (modified from the probes described in [13]), as shown in figure 6. Instead of connecting the probes to an analog spectrum analyzer, in the present configuration the rf signals are digitized at 100 MHz and the Fourier analysis carried out in software. Hence signals up to 50 MHz are meaningful. Probes are located both on the centrepost (high field side) and on the outboard vacuum vessel wall, in both the cases near the midplane. Spectra obtained from both probes are compared in discharges at two different toroidal fields in the figure; peaks are seen at frequencies close to the deuterium fundamental and second harmonic cyclotron frequency evaluated at a major radius near that of the antenna Faraday screens, which are at $R_M = 238$ cm. These peaks would presumably correspond to ion cyclotron quasimodes; the corresponding sidebands are at frequencies higher than can be observed at this digitizing frequency. The peak in the spectra near 2.7 MHz is due to non-linear interaction between the two slightly different FW frequencies applied to the two antenna arrays: one at 114.9 MHz and the other at 117.6 MHz. The peaks in the 40–50 MHz range have not yet been identified. Progress in evaluating the importance of the PDI activity will require observation of such activity in the lower harmonic

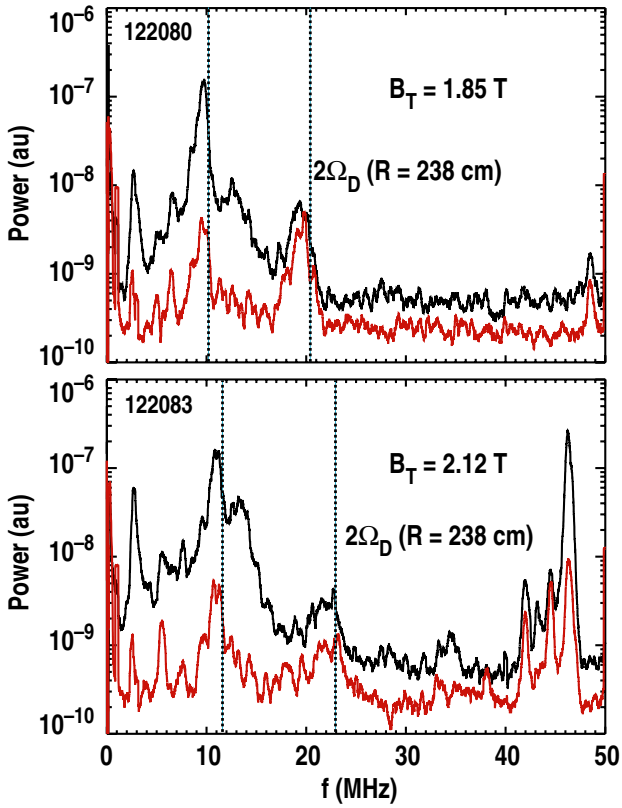

Figure 6. Rf spectra obtained during 8th harmonic heating at two different values of toroidal field: 1.85 T in the first case (which is from the discharge shown in figure 5) and 2.12 T in the second. In each case spectra measured with rf probes on the inboard wall near the midplane (lower amplitude, red curves) and similar probes mounted on the outboard wall near the midplane (higher amplitude, black curves) are shown. Vertical lines indicate the fundamental and 2nd harmonic deuterium ion cyclotron frequency using the magnetic field at a major radius of 238 cm (near the outboard wall).

case and correlation with other manifestations of edge power absorption, such as the edge ion heating seen in the NSTX experiments.

In support of the third possibility (that linear theory is inadequate to describe the experiment), it should be noted that a much more sophisticated non-linear model, based on the combination of the TORIC and ORBIT-RF codes, appears to predict only weak absorption for the 8th harmonic in this experimental condition [19]. Understanding the differences between the results predicted by this model and those of linear theory is the topic of ongoing work. Detailed examination of the results of the non-linear model shows that the interaction at the 8th harmonic occurs almost exclusively for particles near or above the injection energy, in agreement with results from the linear modelling. Hence, the strength of the damping in the final quasilinear state depends sensitively on the size and extent of the tail that is pulled out above the injection energy, and this in turn strongly depends on the magnitude of the rf electric field around the cyclotron harmonic layer. The rf electric field internal to the plasma is not measured and so must be calculated in a model. However, these models do not incorporate the poorly-characterized edge losses, so the electric field values at the resonance layer calculated in these models are likely to be overestimates.

Very recent modelling of these experiments with the GENRAY ray-tracing code combined with the CQL3D bounce-averaged quasilinear Fokker–Planck code indicates sensitivity of the absorption strength to the fast ion spatial diffusion coefficient. With neither edge losses nor radial diffusion in the model, a significant enhancement of the tail above the injection energy is predicted for both 4th and 8th harmonics at realistic rf power levels and corresponding increases in neutron rate for both the cases. Turning on radial fast-ion diffusion in this model (which is an inextricable part of the ORBIT-RF model) decreases the size of the tail above the injection energy and the neutron rate. The effect of sawtooth crashes to redistribute fast ions in the central region may be a related important effect that is not taken into account in either the ORBIT-RF or the CQL3D modelling. In accordance with the results previously found at lower density at 4th harmonic [14], where the fast ion tail and the sawtooth period decreased as the density was raised, no evidence of sawtooth stabilization is seen in the high density L-mode condition of figure 5. While the absence of stabilization may simply be due to the lack of a substantial high-energy tail, it might also be that the timescale on which a tail is pulled out is comparable to or longer than the sawtooth period and the sawtooth crashes periodically reduce the density of fast ions in the resonant region, hindering or preventing the buildup of the tail. Certainly in the low-density regime of [14] the large crashes of the partially stabilized sawteeth reduced the neutron rate virtually to the no-rf value, so that in that case the tail above the injection energy was strongly reduced by sawtooth crashes. A fully self-consistent simulation of the interaction of the fast ions, the FW and the sawteeth, that would incorporate the temporally modulated and spatially non-uniform redistribution of fast ions due to sawtooth crashes, the stabilizing effect of the fast ions on the sawteeth and the buildup of the tail in time has not been attempted. It may be that such an elaborate simulation may be necessary to describe fully the physics of this rapidly-sawtoothing regime; creation of a sawtooth-free period in which to perform the experiment in a simpler case would be difficult at the high density needed to produce sufficiently high values of λ_s for strong 8th harmonic damping, at least at toroidal field values near 2 T. This suggests a future experiment to explore high harmonic damping at lower toroidal field (and at lower FW frequency) in a sawtooth-free period.

4. Summary and conclusions

We have presented a new theoretical form for the linear ion cyclotron harmonic damping of fast Alfvén waves which, though it is equivalent to existing formulations (e.g. [4]), has physical meaning more easily assigned to each term. The use of a Maxwellian distribution to model the SDDF resulting from high power NB injection overestimates the damping strength, and the size of that overestimate grows with harmonic number. A more realistic model of the beam SDDF shows the importance of both the cutoff in the SDDF at the beam injection energy and the anisotropy in velocity space; a strong dependence of the damping strength at high harmonic on the beam injection geometry is predicted. The effects on the cyclotron absorption due to ray propagation

in a toroidal equilibrium have been evaluated and found to be quite significant. The theory predicts that absorption at high ion cyclotron harmonics can be important in discharges at high beta with substantial fast ion populations. Strong 4th and 5th harmonic absorption has been observed in DIII-D L-mode experiments with 60 MHz FW power, with direct evidence of the rf-driven beam acceleration obtained with the Doppler-shifted D_α charge exchange recombination diagnostic. Contrary to linear theoretical expectations, absorption at 7th and 8th harmonics appears to be weak in high density L-mode discharges with 116 MHz fast waves at either of the two available beam injection angles. Understanding the apparent discrepancy is the aim of ongoing study; the subject is relevant not only to experiments combining NBs and fast waves but also to future burning plasma experiments that use FWCD, where parasitic damping on the alpha particles may be an issue.

Acknowledgments

Work supported by the US Department of Energy under Cooperative Agreement DE-FC02-04ER54698, SC-G903402, DE-FG03-86ER53266, DE-AC05-00OR22725, DE-AC02-76CH03073 and DE-FG03-99ER54541.

References

[1] Myra J 2005 *Proc. 16th Topical Conf. on Radio Frequency Power in Plasmas (Park City, Utah, USA, 2005)* (New York: AIP) p 3, 2006 *Nucl. Fusion* **46** at press
[2] Wilson J R *et al* 2005 *Proc. 16th Topical Conf. on Radio Frequency Power in Plasmas (Park City, Utah, USA, 2005)* (New York: AIP) p 66
[3] Petty C C *et al* 1997 *Proc. 12th Topical Conf. on Radio Frequency Power in Plasmas (Savannah, Georgia, USA, 1997)* (New York: AIP) p 225
[4] Stix T H 1992 *Waves in Plasmas* (New York: AIP)
[5] Porkolab M 1992 *Thomas H. Stix Symp. on Advances in Plasma Physics (Princeton, NY, USA, 4–5 May 1992)* (New York: AIP) p 99
[6] Dumont R J, Phillips C K and Smithe D N 2003 *Proc. 15th Topical Conf. on Radio Frequency Power in Plasmas (Moran, Wyoming, USA, 2003)* (New York: AIP) p 439
[7] Cordey J G and Core W G F 1974 *Phys. Fluids* **17** 1626
[8] Cox M and Start D F H 1984 *Nucl. Fusion* **24** 399
[9] Petty C C *et al* 2001 *Plasma Phys. Control. Fusion* **43** 1747
[10] St John H E, Taylor T S, Lin-Liu Y R and Turnbull A D 1994 *Proc. 15th Int. Conf. on Plasma Physics and Controlled Nuclear Fusion Research 1994 (Seville, Spain, 1994)* vol 3 (Vienna: IAEA) p 603
[11] Petty C C *et al* 1995 *Nucl. Fusion* **35** 773
[12] Prater R *et al* 2005 *Proc. 16th Topical Conf. on Radio Frequency Power in Plasmas (Park City, Utah, USA, 2005)* (New York: AIP) p 106
[13] Ikezi H, Pinsker R I, Chiu S C and deGrassie J S 1996 *Phys. Plasmas* **3** 2306
[14] Heidbrink W W *et al* 1999 *Nucl. Fusion* **39** 1369
[15] Heidbrink W W *et al* 2004 *Plasma Phys. Control. Fusion* **46** 1855
[16] http://w3.pppl.gov/transp/
[17] Heidbrink W W 2002 *Phys. Plasmas* **9** 28
[18] Petty C C *et al* 1999 *Nucl. Fusion* **39** 1421
[19] Choi M *et al* 2005 *Proc. 16th Topical Conf. on Radio Frequency Power in Plasmas (Park City, Utah, USA, 2005)* (New York: AIP) p 31, 2006 *Nucl. Fusion* **46** S409–15